Numerical Study of Rotating Detonation Combustor with Backward Facing Step

Qi Sun, Yuechen Hou, Jianping Wang
College of Engineering, Peking University
Beijing, China

1 Physical and Numerical Models

Fig.1 illustrates the physical model of the rotating detonation combustor (RDC) with backward facing step (BFS) used in this research. The RDC is modeled without accounting for the wall thickness, and the BFS is positioned behind the inlet channel. The inner column adopts a tapered guide cone structure. R_{inner} is 20mm and R_{outer} is 25mm. L1, L2, L3 are 3mm, 10mm and 10mm, respectively. The length of RDC is 50mm. This study uses three different models, where the BFS area ratio is adjusted by controlling the bottom radius of the inner column R_{col} equals 5mm, 10mm and 15mm, resulting in ratios ψ of 93.75%, 75%, and 43.75%, where ψ is defined as:

$$\psi = (1 - \frac{A_{col}}{A_{inner}}) * 100\%. \tag{1}$$

The governing equations used in this research are 3D compressible reactive Navier-Stokes equations. Reynolds Averaged Navier-Stokes (RANS) equations combined with the partially stirred reactor (PaSR) are employed, which have been used in our previous work [1]. For each model, the mesh size used in this research is 0.15mm. Although the cellular structure cannot be observed under the current mesh size, the detonation velocity, pressure, temperature, and structural deviations remain relatively small, which is shown in Fig.2 and Table.1. The inlet condition used in this research is based on micro-convergent nozzle, an idealized injection model. To fully capture the impact of BFS on the detonation process, p_0 in this research is set to 6×10^5 Pa, and T_0 is set to 1000 K. Under these conditions, the detonation

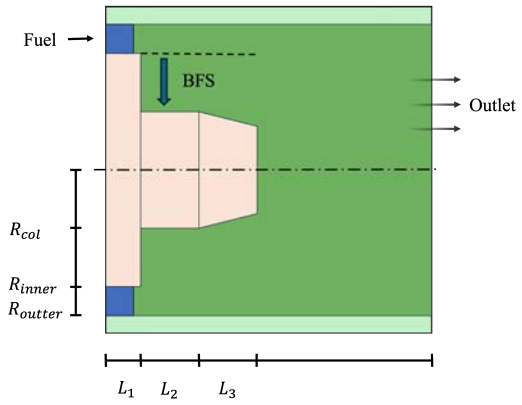

Figure 1: Physical model of RDC with BFS.

Table 1: Comparison of numerical and theoretical results of 1D detonation tube under different equivalence ratios.

ϕ	P_{cal}][atm]	P_{CJ}[atm]	P_{err}[%]	$T_{cal}[K]$	T_{CJ}[K]	T_{err}[%]	U_{cal}[m/s]	U_{CJ}[m/s]	U_{err}[%]
0.6	11.20	11.17	0.27	2613.8	2604.3	0.37	1593.70	1610.87	-1.07
0.8	12.61	12.69	-0.63	2836.9	2853.8	-0.59	1726.37	1714.11	0.72
1.0	13.64	13.77	-0.94	2972.5	2986.8	-0.48	1788.20	1780.71	0.42
1.2	14.59	14.54	0.34	3061.2	3039.4	0.72	1806.35	1823.89	-0.96
1.4	15.10	15.00	0.67	2971.6	2945.3	0.89	1868.16	1846.61	1.17

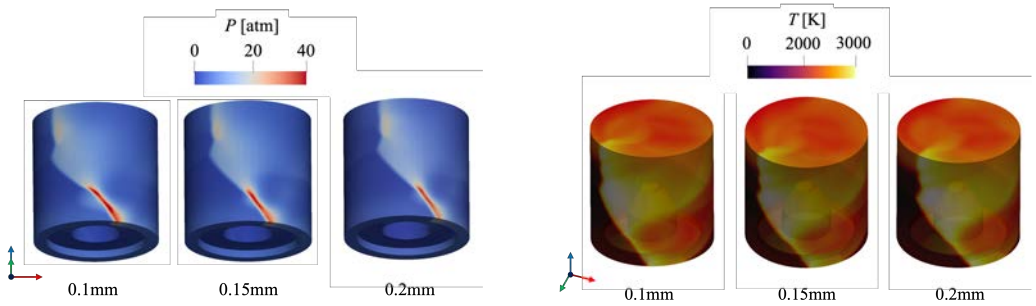

(a) Pressure distribution.

(b) Temperature distribution.

Figure 2: Numerical results of temperature and pressure distributions with different grid sizes.

wave height exceeds the length of the inlet channel L_1. Additionally, the initial pressure p_s in the entire domain is set to 1 bar, with a static temperature T_s of 300 K.

2 Detonation Wave Structure

Fig.3 presents the axial structure of the detonation wave at 460μs after stabilization. At this stage, the detonation wave structure is completely different from the typical detonation configuration. It can be observed that in the presence of BFS, the detonation wave exhibits a very distinct stratification. As shown in Fig.3f ,along the axial direction, the wave can be roughly divided into four distinct zones. Z3 and Z4 primarily develop axially, while Z2 and Z1 exhibit certain tilt angles. The intersection between Z2 and Z3 generates a shock wave that divides the reactants ahead.

Based on the trends in pressure and temperature shown in Fig.4, the detonation wave can be roughly divided into the following subregions, denoted as Z1–X (Z1–1, Z1–2, Z1–3), Z2, Z3 and Z4:

1. Z1-1 (0 – 3 mm). This is the inlet channel, where the pressure gradually increases while the temperature remains relatively stable.

2. Z1-2 (approximately 3 mm – 8 mm). In this region, the temperature begins to drop rapidly, and the pressure, after a slow rise, starts to decrease slightly with only minor variations.

3. Z1-3 (approximately 8mm – 14 mm). Here, the temperature again starts to rise rapidly, gradually approaching the temperature of the inlet channel. The pressure also begins to rise in a wave-like manner and, after reaching a maximum, quickly declines.

4. Z2 (approximately 14 mm – 29 mm). Within this region, both the pressure and temperature of the detonation wave exhibit an overall decreasing trend, followed by a sharp decline near 29 mm, where the minimum values are reached.

5. Z3 (approximately 29mm – 34 mm). In this region, the pressure and temperature gradually begin to rise. And the temperature drops sharply near 34 mm.

6. Z4 (approximately 34mm – 40 mm). In this final region, both the temperature and pressure further increase.

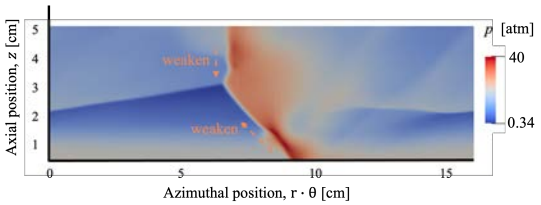

(a) Distribution of pressure in log scale

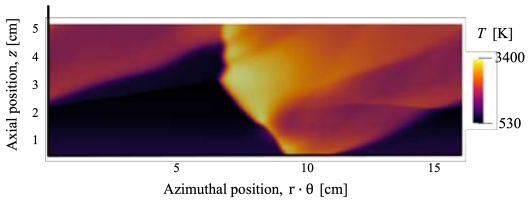

(b) Distribution of Temperature

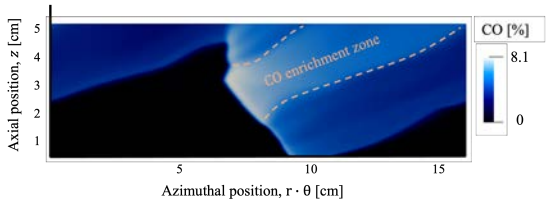

(c) Distribution of CO percentage

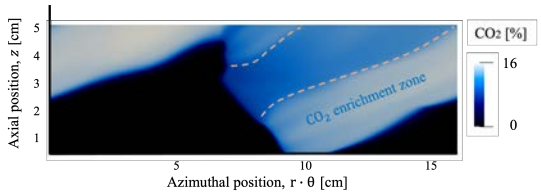

(d) Distribution of CO_2 percentage

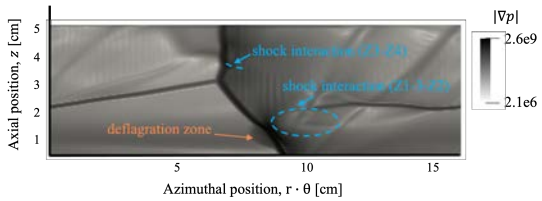

(e) Distribution of pressure gradient in log scale

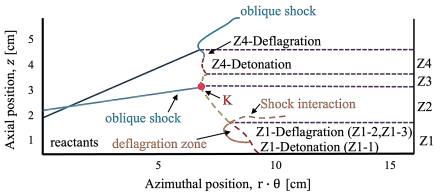

(f) Schematic of detonation wave structure

Figure 3: Physical parameters distribution and schematic of wave structure (Radius: 25mm, t = 460μs, ψ = 50%).

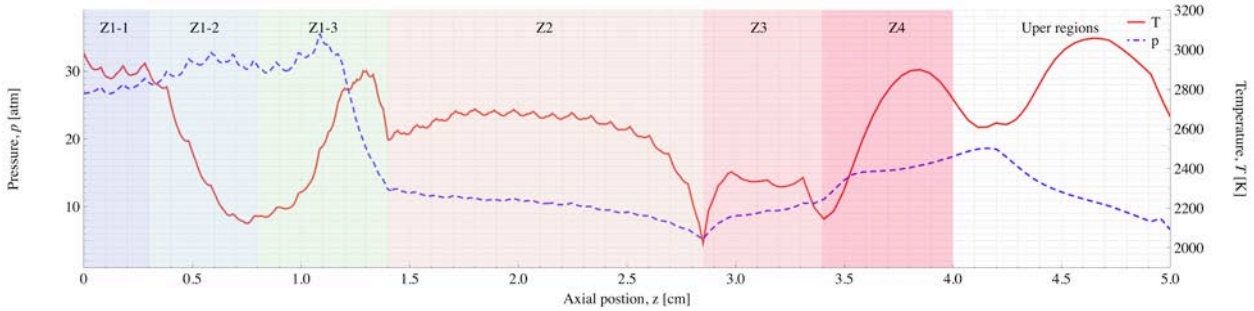

Figure 4: The distribution of pressure and temperature along the detonation wave.

The formation of this structure is closely related to the shock band in the global field, which can be divided into three parts. The first part is a shock naturally formed by the expansion effect induced by BFS. The second part is a shock band produced by the velocity difference between the combustion products and the inlet fuel. And the third part is a derivative of the detonation wave. The formation of this shock band is shown in Fig.5.

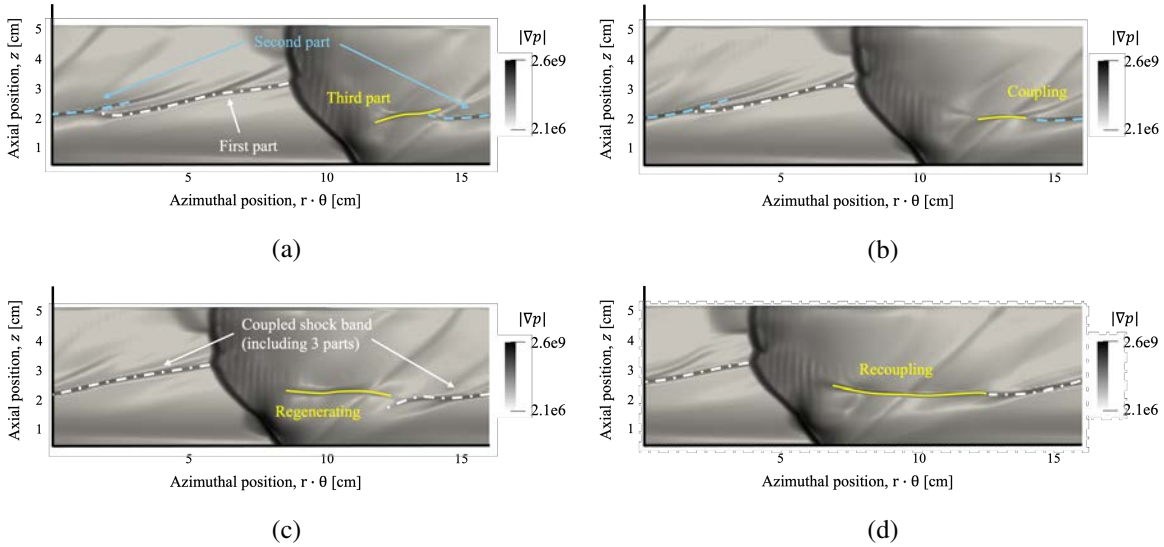

Figure 5: Schemes of generating and coupling process of shock band from 365 μs to 390 μs. (a) 365 μs. (b) 370 μs. (c) 380 μs. (d) 390 μs.

3 Wave System Structure

The presence of BFS leads to a more complex wave system structure within RDC compared to the co-axial RDC and hollow RDC. Fig.6 shows the radial distribution of the wave structure within the combustor at 460μs, after the detonation wave has stabilized. The internal wave structure is primarily composed of diffracted and reflected shock waves, which couple with the detonation wave itself and propagate at the same velocity as the detonation wave.

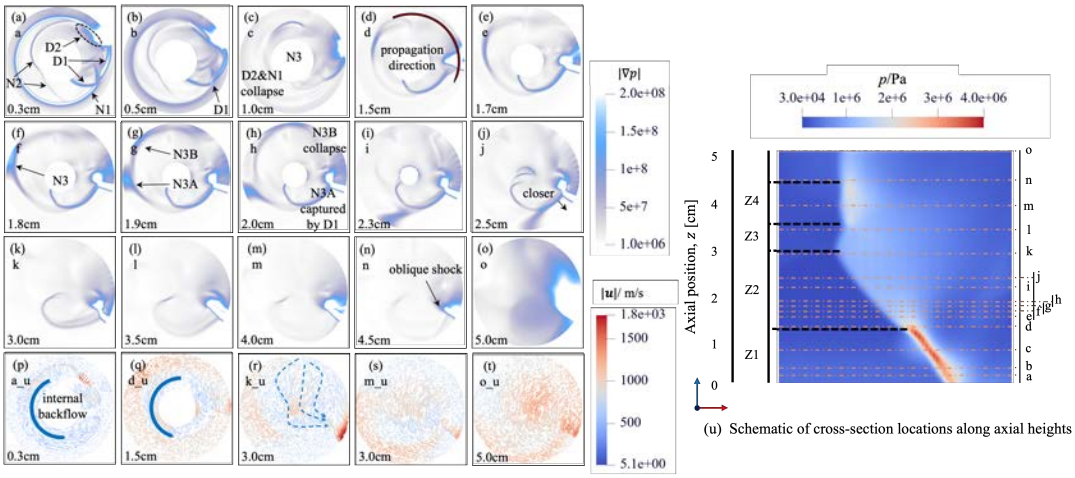

Figure 6: Wave system and flow field structures at different axial height (t = 460μs, ψ = 50%).

Based on their relationship and degree of coupling with the detonation wave, the internal wave structures can be divided into two categories. The first category consists of wave structures that originate from the detonation wave itself, such as structures D1 and D2 shown in Fig.6a. D1 represents the leading shock structure, which is generated by diffracted shock waves emitted by the detonation front. This structure is also present in the hollow RDC [5]; however, unlike in the case of a combustor with an internal column, the D1 structure in an open-ended combustor does not exhibit a precursor phenomenon and

simply follows the detonation wave, decaying toward the center. In the presence of an internal column, D1 evolves into a precursor structure, appearing ahead of the detonation wave and propagating with it. The D1 structure persists as long as the detonation wave exists, as shown in Fig.6a to Fig.6n, where the structure consistently appears at the front of the detonation wave. The intensity of D1 decays both radially and axially, which is influenced by the detonation wave intensity, weakening as the detonation wave weakens. Moreover, the intensity of D1 is sensitive to the internal column. In Fig.6j and Fig.6k, it is evident that, at similar detonation intensities, the D1 structure is significantly stronger when an internal column is present compared to cases without an internal column. Thus, D1 can be considered the result of the diffracted shock wave of the detonation wave being compressed by the internal column in the hollow RDC. Furthermore, the position of D1 is related to the detonation wave itself. In the high-intensity detonation zone, like Z1 and Z4, due to the compression characteristics of the detonation wave, the diffraction point is located closer to the wall, as shown in Fig.6j. In the absence of an internal column, it is more easily induced by the wall, and after the intensity weakens, it generates an inward-reflected shock wave. In weak detonation regions, where the detonation waves compression is less effective, the diffraction point tends to occur closer to the internal column.

The D2 structure, which is a post-shock structure, is more complex and is generated when the detonation wave encounters the BFS, producing reflected shock waves that propagate radially. These waves decay rapidly in the radial direction. This structure is not sensitive to the internal column and exists only during the sudden expansion phase.

The second category of wave structures is directly generated by the flow field and is highly sensitive to the combustor configuration. While these structures do not directly couple with the detonation wave, they are still influenced by it. Examples of such structures include N1, N2, and N3, as shown in Fig.6a and Fig.6f. The N1 structure is generated when the high-pressure inlet flow encounters the BFS and expands inward. This structure affects the D1 structure near the BFS and generates secondary shock waves. However, the height of this structure is relatively low, on the order of millimeters.

The N2 structure is generated by the flow field motion induced by the detonation wave. Fig.6p to Fig.6t show the velocity direction of the flow at different axial heights, revealing that, at all axial positions, the internal flow field consistently exhibits reverse flow relative to the detonation wave. The origin of this flow can be understood as a negative feedback mechanism, where the combustion chamber, which only has axial momentum input, must generate new momentum in the opposite direction to maintain overall momentum conservation. As a result, there is always a reverse velocity component in the internal flow field. The role of N2 is similar to that of D1, as both regulate the flow velocity and direction within the internal flow field. Its height is also relatively low, and as the detonation wave tilts forward along the axial direction, the N2 structure gradually decouples and disappears, giving way to the emergence of the N3 structure.

The N3 structure forms only in weak detonation regions and is essentially a post-shock wave surface derived from the D2 structure. Due to the higher pressure behind the detonation wave, this induces inward radial velocity, creating a shock surface that develops inward from the D2 structure. As the flow field develops circumferentially, this structure begins to decouple from D2 and propagates in the opposite direction. However, without D2 as a driving force, the N3 structure would collapse. As the process progresses, the N3 structure decouples and is induced by the wall into two parts: N3A and N3B, which are shown in Fig.6g. The N3B structure decays due to lack of drive, while N3A is captured by the D1 structure and couples with it to form a secondary D1 structure. However, since the diffraction point of D1 is related to the detonation wave intensity, N3A is only captured in weak detonation regions and disappears as it is compressed by the wall while entering Z3. In some sense, the existence of N3A supplements the speed adjustment under weak detonation, fulfilling part of the D1 function.

4 Effects of Changes in BFS Area Ratio

Fig.7 presents the distributions of pressure and temperature along the detonation wave for ψ values of 43.75% and 93.75%, respectively. Compared to Fig.4, the overall detonation wave structure does not exhibit significant differences, as the main zones Z1Z4 remain present. The most notable difference lies in the relative extents of the Z1 and Z2 regions; with an increasing BFS ratio, the proportion of the Z1 zone gradually increases, while that of the Z2 zone decreases.

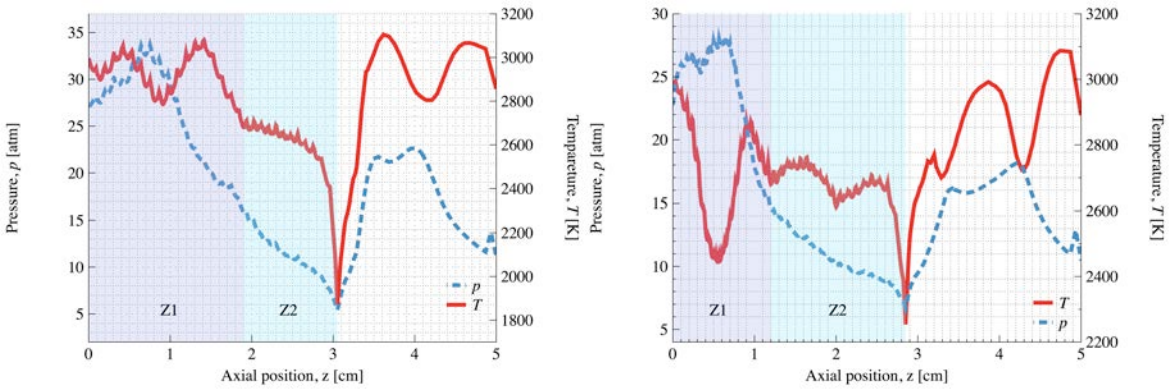

(a) (b)

Figure 7: The distribution of pressure and temperature along detonation waves (t = 460 μs). (a) ψ = 93.75%. (b) ψ = 43.75%.

References

[1] Liu X, Cheng M, Zhang Y. Design and optimization of aerospike nozzle for rotating detonation engine. Aerospace Sci. Tech. 120:107300.

[2] Schwinn KS, Kan B, Sardeshmukh SV. (2017). Self-Excited, multi-kHz dynamics in a linear, semi-Bounded detonation channel. 55th AIAA Aerospace Sciences Meeting.

[3] Liu X, Luan M, Chen Y. (2021). Propagation behavior of rotating detonation waves with premixed kerosene/air mixtures. Fuel. 294: 120253.

[4] Athmanathan V, Braun J, Ayers Z. (2020) Detonation structure evolution in an optically-accessible non-premixed H_2-Air RDC using MHz rate imaging. AIAA Scitech 2020 Forum.

[5] Huang S, Zhou J, (2023) Liu W. Analysis on the radial structure of rotating detonation wave in a hollow combustor. Fuel. 348: 128581.